This journal is © The Royal Society of Chemistry 2014

ELECTRONIC SUPPLEMENTARY INFORMATION (ESI)

Protein-templated gold nanoclusters sequestered within sol–gel thin films for the selective and ratiometric luminescence recognition of Hg^{2+}

Carrie Hofmann,[a] Jeremy B. Essner,[b] Gary A. Baker*[,b] and Sheila N. Baker*[,a]

[a] *Department of Chemical Engineering, University of Missouri–Columbia, Columbia, MO 65211 USA. E-mail: bakershei@missouri.edu*
[b] *Department of Chemistry, University of Missouri–Columbia, Columbia, MO 65211 USA. E-mail: bakergar@missouri.edu*

Experimental

Materials and Reagents

All experiments were carried out using Ultrapure Millipore water (18.2 MΩ cm). Bovine serum albumin (≥98%), gold (III) chloride hydrate (99.999%), sodium hydroxide (≥97%), sodium phosphate dibasic (≥99%), sodium phosphate monobasic (98%–102%), and tetraethyl orthosilicate (TEOS; 99.999% trace metals basis) were purchased from Sigma-Aldrich (St. Louis, MO). Lysozyme type VI was purchased from MP Biomedicals. The chloride salts of Cu^{2+} (lab grade), Fe^{3+} (ACS 97–102%), Sr^{2+} (99+% ACS), Ba^{2+} (>99%), Ca^{2+} (99.999%), and Zn^{2+} (99.99% metals basis) were obtained from Fisher Scientific (Pittsburg, PA). The chloride salts of Ni^{2+} (98%), Hg^{2+} (ACS >99.5%), Na^{+} (ACS ≥99.0%), and Mn^{2+} (99.99% trace metals basis) were purchased from Sigma-Aldrich (St. Louis, MO). All reagents were used in the form received, without subsequent purification. Fisher brand filter paper (coarse porosity, 7 cm diameter), pre-cleaned Fisherbrand borosilicate EPA glass vials equipped with PTFE/silicone septa, and Corning plain glass microscope slides were also obtained from Fisher Scientific.

Synthesis of AuNCs@BSA

The typical synthesis of AuNCs@BSA was completed by combining 1.0 mL of 50 mg/mL BSA dissolved in deionized water with 1.0 mL of 10 mM $HAuCl_4$ (*aq*) at 37 °C under 250 rpm stirring in a precleaned Fisherbrand EPA borosilicate glass vial. After 3 min, 100 μL of freshly prepared 1.0 M NaOH (*aq*) was added. The reaction was allowed to proceed by stirring at 37 °C for 12 h ("conventional route") or under gentle microwave irradiation for 2 h to maintain a temperature of 37 °C under medium stirring using a CEM microwave (Discover SP model). After synthesis, the conventionally prepared AuNCs@BSA exhibited a deep orange hue whilst those prepared by MW irradiation were initially a light yellow color which evolved over time to take on a similar deep orange color. In both instances, immediately after preparation, strong red luminescence was observed under a black light (UV-A: 365 nm). In order to allow for the preparation of more highly concentrated AuNCs@BSA solutions in subsequent sol–gel film work, an aliquot of the as-prepared AuNCs@BSA were flash frozen in liquid nitrogen and immediately freeze-dried on a Labconco FreeZone Plus 4.5L Console Freeze-Dry System ($P \approx 10^{-4}$ bar for 24 h). We note that the FTIR spectra for freshly prepared AuNCs@BSA and an AuNCs@BSA solution reconstituted from the lyophilized material are indistinguishable. Except where noted for quantum yield studies, all AuNCs@BSA solutions and freeze-dried powders were stored in the refrigerator.

In order to determine the extinction coefficient (ε) for the AuNCs@BSA, the concentration of BSA used to generate the clusters was initially found by using ε_{278} = 8,700 M^{-1} cm^{-1}. The corresponding ε_{350} value for AuNCs@BSA was determined from serial dilutions of a dialyzed AuNCs@BSA sample having a well characterized BSA concentration (assuming a 1:1 AuNC:BSA stoichiometry), and is summarized in Fig. 3A.

Sol–Gel-Derived Thin Film Preparation

Tetraethylorthosilicate (TEOS) sol was prepared by combining 2.8 mL of deionized water with 200 μL of 1.0 N HCl followed by dropwise addition to 9.0 mL of TEOS under constant stirring at room temperature using a pre-cleaned EPA glass vial as reaction vessel. The mixture was allowed to hydrolyze for at least 4 h at room temperature while stirring within the capped vial. Starting from the freeze-dried material, a 66 mg/mL AuNCs@BSA solution was prepared in 25 mM phosphate buffer solution (PBS, pH 7.4). A 200 μL aliquot of this AuNCs@BSA solution was combined with 200 μL of the pre-hydrolyzed TEOS sol and the mixture pipetted onto a prepared glass slide with dimensions of ~1.0 cm × 2.5 cm. We note that, after being cut to the desired dimensions, glass slides were prepared in advance of this step by soaking in 0.1 M NaOH, rinsing exhaustively under deionized water, and drying in a dry, filtered nitrogen stream. The buffered AuNCs@BSA/sol mixture was then spin coated onto glass slides using a Specialty Coating Systems 6800 Spin Coater. Spin coating proceeded for 30 s at 2000 rpm. The thin films were allowed to set for 5 min after spin casting and allowed to age at least 2 days in 25 mM PBS (pH 7.4) at 4 °C in the dark. Profilometry experiments showed that the aged sol–gel films were typically 1.0 ± 0.1 μm thick.

Characterization

Optical Absorbance:

Absorbance measurements were performed on a Shimadzu UV-2401 PC UV–Vis recording spectrophotometer using a medium scan rate with 1 nm intervals and a slit width of 5 nm. Samples were diluted with deionized water in quartz cuvettes having a 1-cm path length. All spectra were appropriately blank corrected.

Fluorescence Studies:

Steady-state fluorescence studies were performed on a T-format FluoroLog®-3 spectrofluorimeter (HORIBA Scientific; model FL3-22) equipped with double-grating monochromators in the excitation and emission channels using excitation and emission slit widths of 5 nm. Typically, samples were prepared by diluting 100 μL of as-prepared AuNCs@BSA with 2.5 mL of deionized water in quartz cuvettes with a 1-cm path length. Spectra were background corrected using the appropriate solvent. Quantum yields were obtained by diluting the AuNCs@BSA sample to an optical density of 0.015 at a wavelength of 488 nm. The sample was excited at 488 nm and compared to rhodamine 6G (R6G) in ethanol (Φ_R = 95%) with a similar optical density. Fluorescence quantum yields (Φ_f) were calculated using the equation:

$$\Phi_f = \Phi_R\left(\frac{I}{I_R}\right)\left(\frac{A_R}{A}\right)\left(\frac{n^2}{n_R^2}\right)$$

where the *R* subscript denotes the reference (i.e., R6G), Φ is the fluorescence quantum yield, *I* is the relative fluorescence intensity, A is the absorbance at the excitation wavelength, and *n* is the refractive index of the solvent used.

DLS/Zeta Potential Measurements:

Dynamic light scattering (DLS) and zeta potential measurements were performed using a DelsaNano HC (Beckman Coulter, Inc.). All samples for measurements were prepared by diluting 0.5 mL of AuNCs@BSA in 4.5 mL of deionized water followed by filtration through a 0.45-μm sterile nylon syringe filter. Size measurements were performed using a disposable polyacrylate plastic cuvette with a 1-cm path length. Zeta potential measurements were performed using a disposable zeta cell and a voltage of 60 V. Analysis was carried out using a one peak Lorentzian fit with a Smoluchowski conversion equation. Size analysis was completed using a noise threshold of 0.3% with an optimum intensity of 30,000 cps and a pinhole size of 50 μm. A normalized second order autocorrelation function, *G*(2), fitting range was used and a volume distribution was collected. All measurements were repeated at least three times.

FTIR Spectroscopy:

All FTIR measurements were performed on a Nicolet 4700 equipped with a Thermo Smart Performer germanium crystal ATR attachment from Thermo Scientific. The resolution was 6 cm^{-1} and 36 scans were performed on each sample. AuNCs@BSA was used as prepared. BSA concentrations were diluted with deionized water such that the protein concentration in the free protein solution was the same as that in the AuNCs@BSA solution.

Metal Ion Detection

***AuNCs@BSA in PBS*:** Ion sensing was completed by diluting 100 μL of AuNCs@BSA in 2.5 mL of 25 mM PBS at pH 7.4. The emission spectra were collected at ion concentrations of 0, 5, 25, 50, 75, 100, 250, 500, 750, and 1000 μM using 350 nm excitation and excitation and emission slit widths of 5 nm. All samples were background corrected using PBS.

***AuNCs@BSA Entrapped within Sol–Gel Thin Films*:** Ion sensing was completed by placing a thin film supported on a glass slide into a quartz cuvette containing a known volume of PBS. Emission spectra were collected at ion concentrations of 0, 5, 10, 15, 25, 50, 100, 250, and 500 μM using 350 nm excitation and excitation and emission slit widths of 5 nm. An equilibration time of 40 minutes was used between measurements. All samples were background corrected using a blank thin film containing no AuNCs@BSA immersed in PBS.

AuNCs@BSA Immobilized on Paper Strips: Sensory paper strips were prepared by first cutting cellulosic filter paper into ca. 1 cm wide strips, followed by a 2 h soaking in 2.5 mL of AuNCs@BSA solution formed by dilution of 1.0 mL of as-prepared (MW-assisted, aged 4 to 5 days; this gives the optimal Φ_f as shown in Fig. 2) AuNCs@BSA with another 1.5 mL of deionized water. The filter paper strips were then removed and allowed to air dry overnight. To test AuNCs@BSA reagent strips, 10 μL of deionized water, 0.1 mM, 1.0 mM, and 50.0 mM ion solutions were

directly pipetted onto the filter paper strips at different locations. Changes in the fluorescence emission were then visualized under handheld UV-lamp illumination at 365 nm.

Table S1 Recovered parameters for modified (two-site) Stern–Volmer fits to the luminescence quenching profiles monitored at 415 nm and 630 nm for AuNCs@BSA in phosphate buffer (PBS) versus sol–gel thin films (SG).

Peak (nm)	f_1	K_{SV1} (M^{-1})	f_2	K_{SV2} (M^{-1})	$<K_{SV}>$ (M^{-1})	r^2
415_{PBS}	0.81	3.47×10^3	0.19	~0	2.80×10^3	0.989
415_{SG}	0.35	5.10×10^4	0.65	600	1.84×10^4	0.993
630_{PBS}	0.99_4	4.88×10^6	0.00_6	~0	4.65×10^6	0.887
630_{SG}	0.97	4.55×10^6	0.03	~0	4.41×10^6	0.961

Table S2 Various Hg^{2+} detection methods and their associated limits of detection (LODs).

Analytical method	Hg^{2+} LOD	Reference
Liquid chromatography (LC)	0.5 ng	[1, 2]
Capillary electrophoresis (CE)	1.1 µM	[3]
"Turn-off" (fluorescence)	2–300 nM	[4-7]
"Turn-on" (fluorescence)	20–60 nM	[8-11]
Ratiometric (fluorescence)	10–100 nM	[12-14]
Colorimetric (small molecule)	10 nM–10 µM	[15-18]
Biomolecular (recombinant whole-cell, protein, oligonucleotide, DNAzyme, or antibody-based)	2.4–40 nM	[19-22]
Miscellaneous materials (fluorescence quenching using various polymers, films, membranes, fibers, nanoparticles)	0.5–330 nM	[23-26]
LC- or GC-ICP-MS	24.9 fM–364 pM	[27-31]
Current approach	0.6–2.5 nM	—

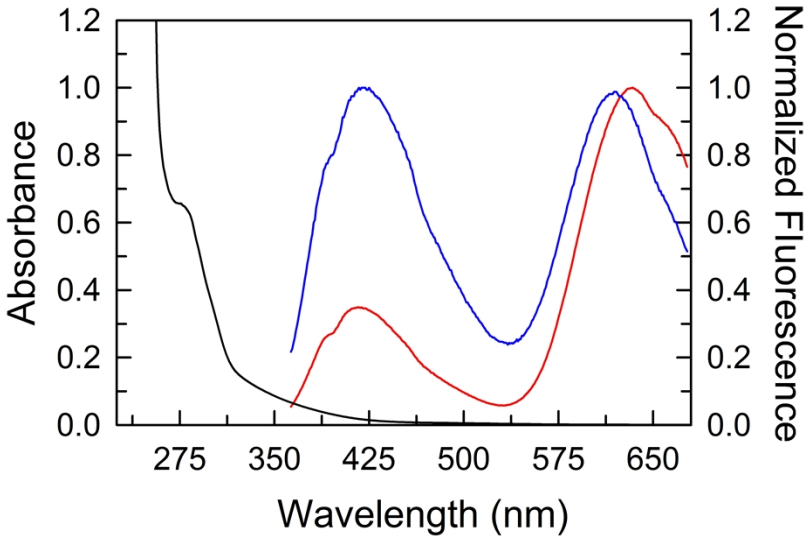

Fig. S1 The absorbance spectrum of AuNCs@BSA in 25 mM PBS at pH 7.4 (black curve). Normalized fluorescence spectra of AuNCs@BSA in PBS (red spectrum) and after entrapment within sol–gel-derived thin films immersed in PBS (blue spectrum).

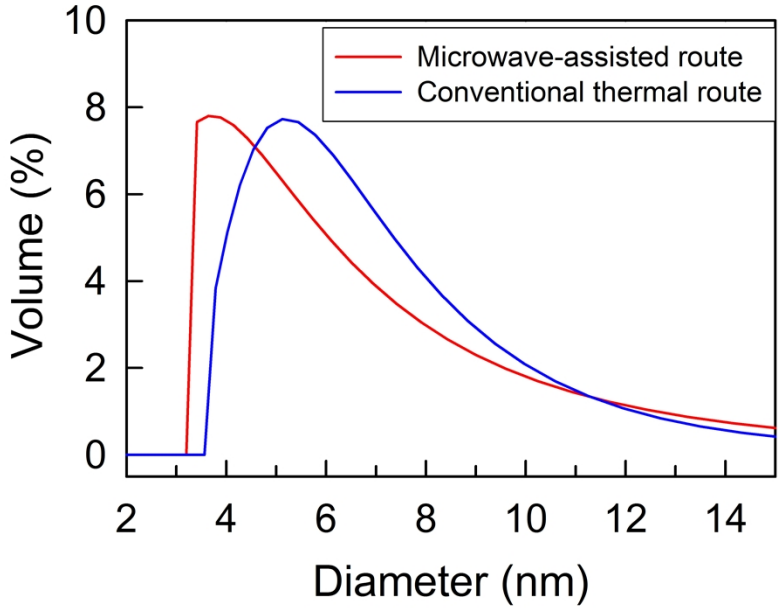

Fig. S2 Size distribution data, as ascertained by DLS experiments, for AuNCs@BSA prepared by conventional heating (blue profile) versus a microwave-assisted route (red profile).

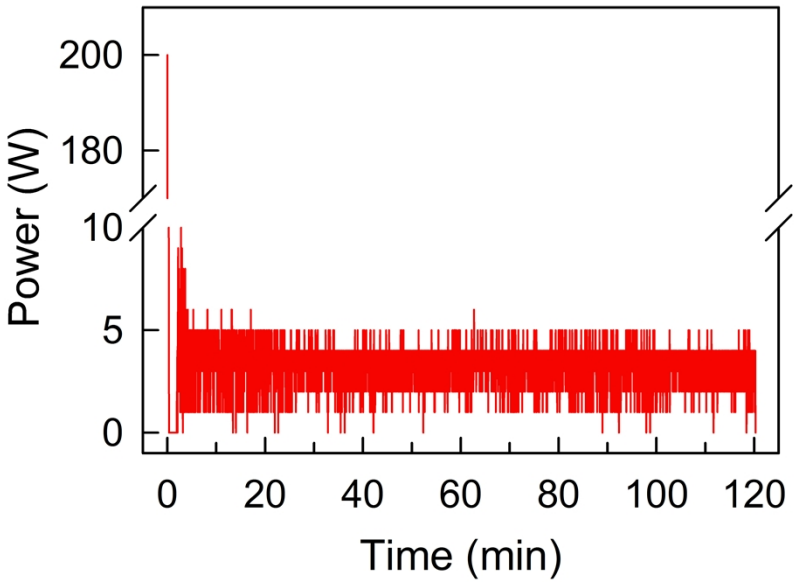

Fig. S3 CEM microwave (Discover SP model) power required to maintain a sample temperature of 37 °C over the course of the 2 h microwave-assisted preparation of AuNCs@BSA. After an initial spike to bring the sample to temperature, the applied power dropped precipitously to 3.2 ± 1.1 W, equivalent to an integrated microwave energy of only 6.4×10^{-3} kWh for the entire reaction.

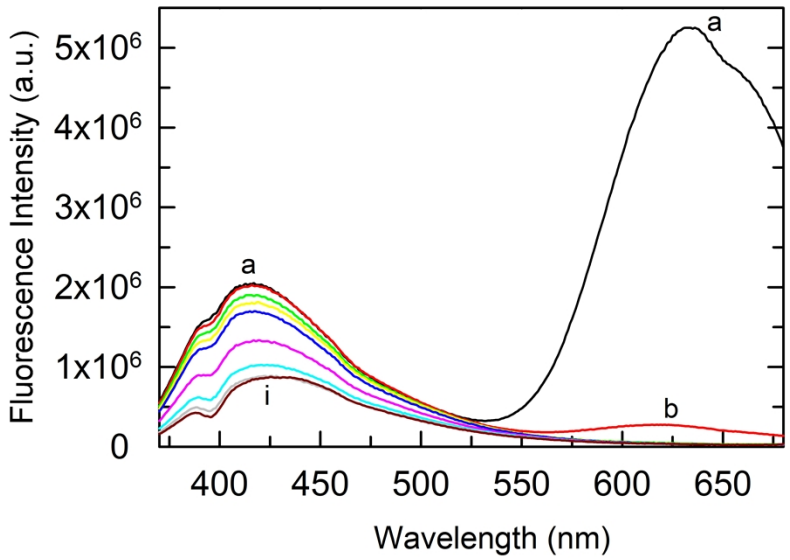

Fig. S4 Emission spectra revealing the differential rates of fluorescence quenching for the "blue" (oxidized BSA) and "red" (Au_{25} nanocluster) bands of AuNCs@BSA in PBS (25 mM, pH 7.4) with incremental addition of Hg^{2+} at these micromolar concentrations: (a) 0, (b) 25, 50, 75, 100, 250, 500, 750, and (i) 1000 μM.

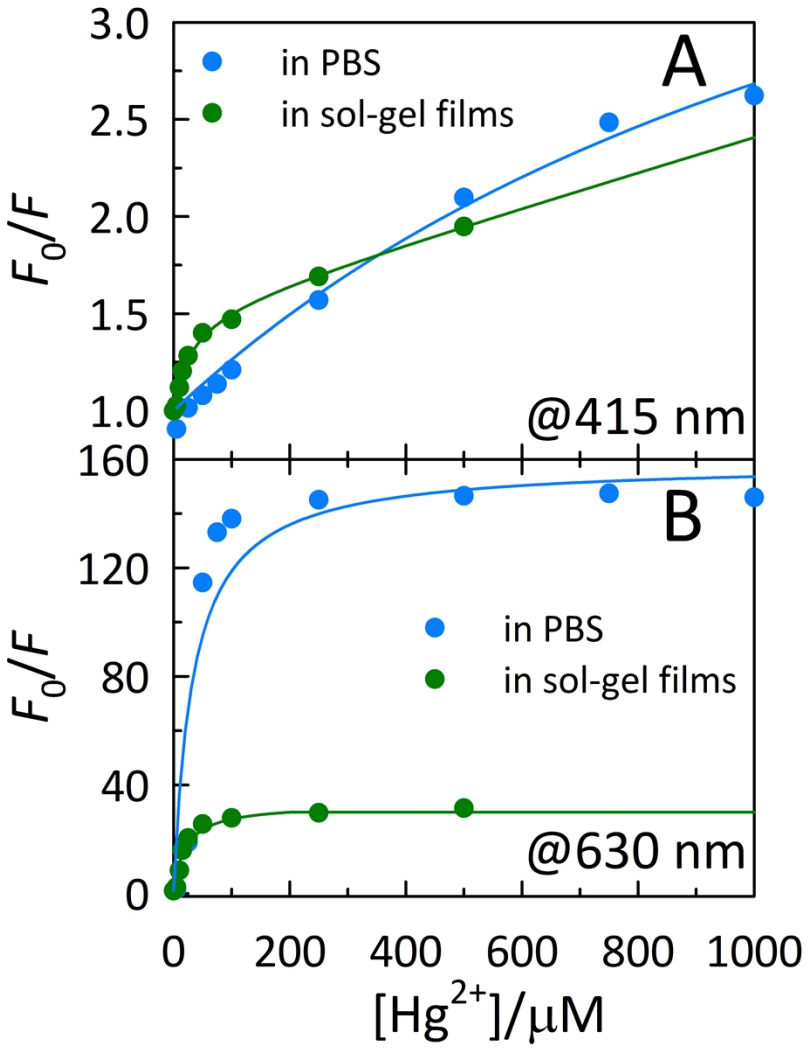

Fig. S5 Stern–Volmer plots for Hg^{2+} quenching monitored at the (A) blue and (B) red emission peaks centered near 415 and 630 nm, respectively, for AuNCs@BSA freely dissolved in PBS versus nanosensor entrapment within sol–gel-derived SiO_2 thin films. The solid lines represent fits to eqn. (1), the Demas model for "two-site" quenching.[32] A two-site quenching model is appropriate if we consider a heterogeneous host matrix in which an ensemble of luminophores encounters essentially two discrete environments and might be expected *a priori* in such instances. In such a scenario, each luminophore population displays an associated quenching constant characteristic of its distinct site. The recovered Stern–Volmer quenching constants associated with the two discrete environments experienced by AuNCs@BSA are captured in Table S1.

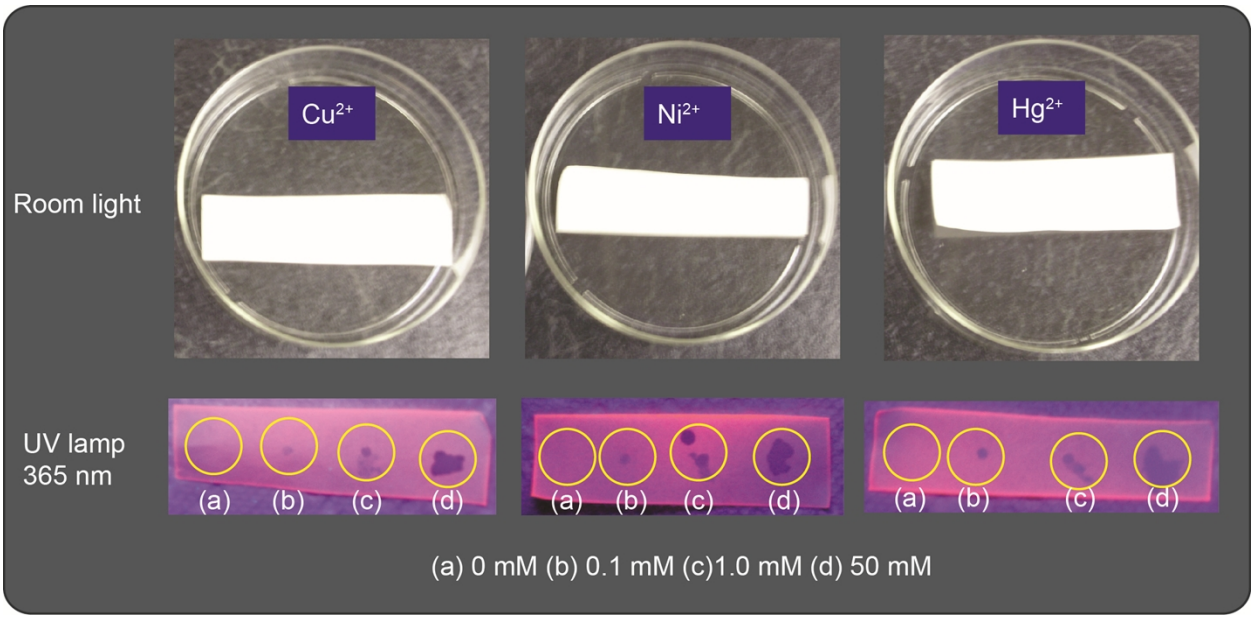

Fig. S6 Images of AuNCs@BSA-impregnated filter paper strips under ambient lighting (top) and a handheld 365 nm UV lamp (bottom) after spotting with solutions of increasing ion (left: Cu^{2+}, middle: Ni^{2+}, right: Hg^{2+}) concentration; from the left of the strip toward the right: (a) 0 mM, (b) 0.1 mM, (c) 1.0 mM, and (d) 50 mM.

References

1. L. Liu, Y.-W. Lam and W.-Y. Wong, *J. Organomet. Chem.*, 2006, **691**, 1092-1100.
2. E. Unterreitmaier and M. Schuster, *Anal. Chim. Acta*, 1995, **309**, 339-344.
3. S. Saito, S. Sasamura and S. Hoshi, *Analyst*, 2005, **130**, 659-663.
4. X.-J. Zhu, S.-T. Fu, W.-K. Wong, J.-P. Guo and W.-Y. Wong, *Angew. Chem. Int. Ed.*, 2006, **45**, 3150-3154.
5. R. Métivier, I. Leray and B. Valeur, *Chem.-Eur. J.*, 2004, **10**, 4480-4490.
6. M.-H. Ha-Thi, M. Penhoat, V. Michelet and I. Leray, *Org. Lett.*, 2007, **9**, 1133-1136.
7. R. Yang, K. a. Li, K. Wang, F. Liu, N. Li and F. Zhao, *Anal. Chim. Acta*, 2002, **469**, 285-293.
8. G. Zhang, D. Zhang, S. Yin, X. Yang, Z. Shuai and D. Zhu, *Chem. Commun.*, 2005, 2161-2163.
9. H. Zheng, Z.-H. Qian, L. Xu, F.-F. Yuan, L.-D. Lan and J.-G. Xu, *Org. Lett.*, 2006, **8**, 859-861.
10. S. Yoon, A. E. Albers, A. P. Wong and C. J. Chang, *J. Am. Chem. Soc.*, 2005, **127**, 16030-16031.
11. X.-M. Meng, L. Liu, H.-Y. Hu, M.-Z. Zhu, M.-X. Wang, J. Shi and Q.-X. Guo, *Tetrahedron Lett.*, 2006, **47**, 7961-7964.
12. Z. Wang, D. Zhang and D. Zhu, *Anal. Chim. Acta*, 2005, **549**, 10-13.
13. L. Feng and Z. Chen, *Sensor Actuat. B-Chem*, 2007, **122**, 600-604.
14. E. M. Nolan and S. J. Lippard, *J. Am. Chem. Soc.*, 2007, **129**, 5910-5918.
15. M. J. Choi, M. Y. Kim and S.-K. Chang, *Chem. Commun.*, 2001, 1664-1665.
16. O. Brümmer, J. J. La Clair and K. D. Janda, *Org. Lett.*, 1999, **1**, 415-418.
17. J. V. Ros-Lis, R. Martínez-Máñez, K. Rurack, F. Sancenón, J. Soto and M. Spieles, *Inorg. Chem.*, 2004, **43**, 5183-5185.
18. J. V. Ros-Lis, M. D. Marcos, R. Mártinez-Máñez, K. Rurack and J. Soto, *Angew. Chem. Int. Ed.*, 2005, **44**, 4405-4407.
19. S. V. Wegner, A. Okesli, P. Chen and C. He, *J. Am. Chem. Soc.*, 2007, **129**, 3474-3475.
20. A. Ono and H. Togashi, *Angew. Chem. Int. Ed.*, 2004, **43**, 4300-4302.
21. M. Matsushita, M. M. Meijler, P. Wirsching, R. A. Lerner and K. D. Janda, *Org. Lett.*, 2005, **7**, 4943-4946.
22. J. Liu and Y. Lu, *Angew. Chem. Int. Ed.*, 2007, **46**, 7587-7590.
23. D. Y. Sasaki and B. E. Padilla, *Chem. Commun.*, 1998, 1581-1582.
24. R. Metivier, I. Leray, B. Lebeau and B. Valeur, *J. Mater. Chem.*, 2005, **15**, 2965-2973.
25. B. Chen, Y. Yu, Z. Zhou and P. Zhong, *Chem. Lett.*, 2004, **33**, 1608-1609.
26. J.-S. Lee, M. S. Han and C. A. Mirkin, *Angew. Chem. Int. Ed.*, 2007, **46**, 4093-4096.
27. Q. Tu, W. Johnson Jr and B. Buckley, *J. Anal. Atom. Spectrom.*, 2003, **18**, 696-701.
28. A. Castillo, A. F. Roig-Navarro and O. J. Pozo, *Anal. Chim. Acta*, 2006, **577**, 18-25.
29. I. Cattani, S. Spalla, G. M. Beone, A. A. M. Del Re, R. Boccelli and M. Trevisan, *Talanta*, 2008, **74**, 1520-1526.
30. W. R. L. Cairns, M. Ranaldo, R. Hennebelle, C. Turetta, G. Capodaglio, C. F. Ferrari, A. Dommergue, P. Cescon and C. Barbante, *Anal. Chim. Acta*, 2008, **622**, 62-69.
31. B. Jackson, V. Taylor, R. A. Baker and E. Miller, *Environ. Sci. Technol.*, 2009, **43**, 2463-2469.
32. G. A. Baker, B. R. Wenner, A. N. Watkins and F. V. Bright, *J. Sol-Gel Sci. Technol.*, 2000, **17**, 71-82.